Carbon Trends 7 (2022) 100165

Contents lists available at ScienceDirect

Carbon Trends

journal homepage: www.elsevier.com/locate/cartre

Carbon nanofabric: A multifunctional fire-resistant material

Vianessa Ng*, Guangfeng Hou, Jay Kim, Gregory Beaucage, Mark J. Schulz*

Department of Mechanical and Materials Engineering, University of Cincinnati, Cincinnati, OH 45221, United States

ARTICLE INFO

Article history:
Received 2 August 2021
Revised 9 February 2022
Accepted 9 February 2022

Keywords:
Carbon Hybrid Materials
Nanofabric
Flame-Resistant
Filterant

ABSTRACT

This paper describes the characterization of carbon nanotube fabric or nanofabric. The nanofabric, has five fundamental properties: light weight, hydrophilic or hydrophobic, flame resistance, flexibility, and filterant. The nanofabric is formed by injecting a precursor aerosol into a high-temperature flow-through reactor. Nanofabric is collected on a drum from the exhuast. Hybrid nanofabric is synthesized by co-injection of a granulated carbon aerosol. Current fabrics used in firefighting might be supplemented with nanofabric or hybrid nanofabric to alleviate the dangers of airborne toxic chemicals and particles, along with assisting in heat management. The nanofabric survived longer in a flame test compared to traditional flame-resistant textiles.

1. Introduction

Firefighter (FF) deaths caused by heat exposure and cancer [1] have been increasing due to the fire environment and the toxicity of combustion products. This has increased interest among personal protective equipment (PPE) manufacturers and fire departments in the functional properties of FF garments. FFs are exposed to carcinogens from airborne particles [2], which could settle and contaminate PPE [3]. Accumulation of carcinogenic particles over time may lead to various health problems. The National Institute of Occupational Safety and Health (NIOSH) initiated its first multi-year study of 30,000 US FFs, from San Francisco, Chicago, and Philadelphia to better understand the potential link between firefighting and cancer. The study completed in 2015 [4, 5] concluded that FFs show higher rates of certain types of cancer than the general US population [5]. Based on this study; (i) FFs had a greater number of cancer-related deaths; and (ii) the likelihood of cancer death increased with the number of fire responses. This has been related to toxic chemicals and smoke particles from the fire which s the FF garments, contact skin, and chemicals being inhaled after FF leave the fire and remove the SCBA mask.

Traditional materials used to manufacture FF apparel like Kevlar, Nomex [6, 7] and Polybenzimidazole (PBI) [8] were developed over 40 years ago. The decomposition temperature, which is the temperature at which a material chemically breaks down caused by heat, of PBI is 1300°F (704 °C), greater than that of Kevlar and Nomex, 1100°F (583 °C) and 700°F (371 °C), respectively [9]. The purposes of these garments are to safeguard FFs against projectiles, punctures, fires, and toxic chemicals. However, these materials have advantages and limitations (listed in **Table 1**). For example, FF's PPE protects the wearer from heat generated by the fire, but it can also simultaneously insulate their bodies preventing metabolic heat from dissipating to the surrounding environment [10].

Kevlar, Nomex, and PBI fibers and combinations thereof resist fire, abrasion, and spillage, but have limitations to effectively dissipate heat or filter airborne, carcinogenic particulates. Previous studies [13–20] have indicated that current protective equipment can contribute to health related heat-stress problems or death. Hence, there is a need to improve high temperature fibers and fabrics to protect FFs from all environmental hazards (resisting heat and filtering toxic chemicals and particles). FF garments should also be as lightweight and flexible as possible.

Since the emergence of nanomaterials (materials with nanoscale components), there has been interests, there has been interest and advancement of carbon nanotubes (CNTs) to exploit their electrical, thermal, mechanical, and optical properties for use in medicine, batteries, water filtration, etc. Thus, CNTs potentially are an auspicious substitute for traditional materials. Janas et al. reported that a free-standing CNT film [21] could be produced from industrially commercial nanomaterial. The CNT film was prepared from a solution consisting of commercial multi-wall CNT (MWCNT) powder and ethyl cellulose, acting as a binder, dissolved in isopropanol. The authors showed that the free-standing CNT lasted as long as Kevlar in a 30 sec (s) flame test. Thus far, similar studies [22–24] have reported CNTs as an alternative

* Corresponding authors.
E-mail addresses: ngva@mail.uc.edu (V. Ng), mark.j.schulz@uc.edu (M.J. Schulz).

https://doi.org/10.1016/j.cartre.2022.100165

Table 1
The benefits and limitations of FF's garments.

Advantages	Disadvantages
Thermal Protection (to prevent heat transfer from the fire environment to the body) [10];	Discoloration of the PPE occurs at temperatures above 180°F/~80 °C [7, 11];
	Moisture in PPE conducts heat rapidly [10];
	Delays awareness of increasing body temperature [10];
Protect against hazardous liquids [10];	FF garments are not tailored to the user's exact measurements [10];
Cut/Abrasion Resistant [10];	In a flashover, the PPE will provide the wearer only 15 s of protection [12];
Heat/Flame Resistant ((PBI up to 1300 degree F (704 degree C));	Difficulty to don/doff gloves when wet;
	Shrinkage of fabric occurs at temperatures exceeding 160°F/70 °C [7, 11];

material in flame retardants. To our knowledge, unaltered CNTs have not been comprehensively tested as a viable flame-resistant material. According to the American Society for Testing Materials (ASTM) [25], the difference between flame retardant and flame resistant is that flame resistant is "a material whereby combustion is prevented, terminated, or inhibited following the application of a flaming or nonflaming source of ignition." Fire retardants are "a chemical used to impart flame resistance" or "coatings to decrease flame spread". Therefore, this paper focuses on developing a flame resistant, hybrid nanofabric that may become a new standard material for thermal protective garments with an increase in performance properties. Nanofabric offers five key performance properties which include the following: 1) hydrophobic or hydrophillic, 2) lightweight, 3) high flexibility, 4) flame resistance, and 5) the ability to filter particulates (Fig. 1). Nanofabric is hydrophobic. Hybrid nanofabric can be hydrophilic.

Nanofabric is proposed to be used to minimize the health risks of FFs and maximize safety for any type of fire incidents (structural and wildland firefighting, industrial, aircraft, and other fires). Additionally, there is a gap in the knowledge of evaluating nanotube fabric for flame resistance and toxic gas filtering applications. This study will include synthesis of two types of nanofabric: (i) pristine nanofabric made entirely of CNTs; and (ii) hybrid nanofabric where CNTs are combined with nanoparticles or microparticles (e.g., granular activated carbon, GAC), which will customize certain material properties of the fabric. The safety of nanofabric will also be evaluated in terms of material combustion (and its by-products). Testing has demonstrated that; (i) pristine nanofabric doesn't shed particles; and (ii) when burned, carbon dioxide (CO_2) is released as a by-product.

2. Materials and methods

2.1. Materials

The fabrication of nanofabric begins with the synthesis of CNTs via gas phase pyrolysis. A customized reactor was developed with (i) a high gas flow rate; (ii) high temperature (1400 °C); (iii) short residence time; and (iv) innovative venturi fuel and particle injector. Under atmospheric pressure, liquid feedstock solution (containing ferrocene and thiophene dissolved in methyl alcohol and n-hexane) is horizontally injected into a ceramic tube from the left-side of the reactor and the produced CNT web or sock is collected on a drum on the right-side of the reactor (shown in **Fig. 2**). This process is cited in our previous work [26, 27].

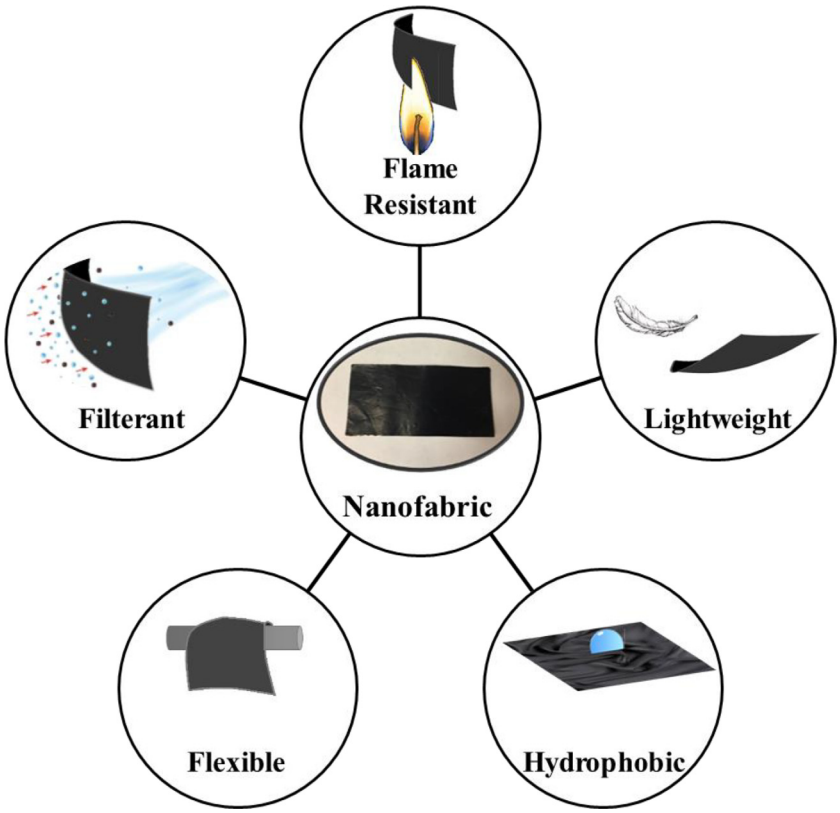

Fig. 1. Fundamental performance properties of nanofabric.

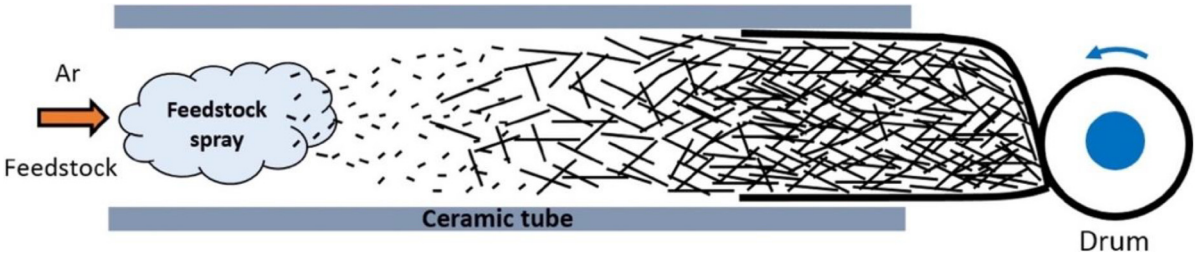

Fig. 2. Illustration of the experimental set-up for CNT synthesis [27].

Hybrid nanofabric is made by injecting granulated carbon in the synthesis process described above. Nanofabric sheets, pristine and hybrid (embedded with granulated activated carbon (GAC), (CNT-GAC), were synthesized via gas phase pyrolysis.

In addition to nanofabric and hybrid nanofabric, traditional flame-resistant sample textiles were investigated as supplied by PBI Performance Products, Inc and TexTech Industries were tested. PBI Max 7.0, TenCate Quantum4i, Glide with PBI G2, and Z-Flex P202 are the fabric swatches supplied by PBI Performance Products and are primarily used in FF PPE. The swatches are made of two to three layers; each a combination of PBI and an aramid blend (Kevlar and/or Nomex). High-performance, non-flammable fabrics from TexTech Industries were ResistX and CarbonX, which are modacrylic, cotton, and nylon jersey fabric. Cotton fabric (Waverly Inspiration, 100% cotton) was tested as a control baseline sample. Additional testing data is provided in Supporting Information.

2.2. Testing methods of materials

Simple screening tests were performed to qualitatively show the relative performance of the different materials. The pristine nanofabric was used in all tests (as described below), while pristine with GAC (hybrid) was only tested in the filtering experiment.

2.2.1. Flammability test

Flammability testing was performed to measure how easily a material burn. The samples were mounted and supported with clamps, positioned horizontally from a controlled flame. The tip of the flame from a propane torch was placed 76 mm away from the surface of the sample. The flame was kept on until it burned through the sample. The maximum temperature and burning time were recorded.

2.2.2. Filtration efficacy test

A filter test bed was designed to qualitatively determine the "capture" of particulates. The sample was placed inside a N95 disposable respirator attached to the 7.62 cm round duct of a 19.05 cm (L) x 19.05 cm (W) x 10.16 cm (D) exhaust fan. A metal grating was placed on the exhaust fan to ensure safety and to allow flow through. A piece of 2 cm (L) x 2 cm (W) plastic was placed inside of the ceramic bowl, which was 63.5 mm away from the fan. The plastic was burned with a butane lighter for two minutes (min). A FLIR T660 thermal infrared camera was used to video the flow of smoke.

2.2.3. Wettability test

Wettability was measured by the water contact angle test (ASTM D7334–08 [28]) using 5 microliter (μL) of water on a Kruss drop shape analyzer DSA25E instrument at room temperature. For samples that are hydrophilic and unable to determine the contact angle, a wettability test was performed. Using a stopwatch, the time was measured from the moment the droplet was released to the moment it was absorbed. This was performed five times. The average time was reported. For extremely hydrophilic samples (contact angle $< 0°$), a video was recorded.

2.3. Characterization

Various non-destructive testing methods were used to characterize the surface morphology and material properties of each sample. A Renishaw in via Raman spectroscope with an Argon laser of 514 nm and 785 nm wavelength was used to measure the graphitic/disorder (G/D) ratio which is a measure of quality of the material. Data was collected for the CNT samples at multiple spots. The average was used for the data analysis. A Thermo Scientific Apreo C LoVac scanning electron microscope (SEM) was used to image and verify fabrication of CNT, surface morphology framework, and thickness. All nonconductive samples were sputter coated for 90 s with palladium using a Denton Vacuum Desk V.

3. Results and discussion

The performance of CNT sheets was characterized using Raman spectroscopy and SEM. Additionally, flame and air filtration testing were performed to determine the material's thermal performance and chemical absorption. CNTs produced using gas phase pyrolysis aggregate to form bundles that intertwine with other bundles. **Fig. 3** shows pristine CNT fabric and hybrid nanofabric.

Fig. 3a is an image of the hybrid sheet produced, which measured 8.86 cm (L) by 3.81 cm (W). Visually, there is no difference in appearance between pristine CNT and hybrid CNT sheets. A microscopic image using SEM is shown in **Fig. 3b**. The sheet is comprised of CNTs and GAC particles integrated together in the CNT sheets.

3.1. Flame testing

A horizontal flame test was performed, using a propane torch (~2000 °C) on different samples with varying thicknesses. The tip of the flame was set at 76 mm from the sample which was clamped between microscope slides and mounted on a stand (shown in **Fig. 4**). The samples were individually and continuously heated and timed until the flame burned through the material. The time it took the sample to burn-through was recorded.

Table 2 compares the burn-through test results of eight different types of fire-resistant fabrics and nanofabric. Sample 1 is cotton used as a control. Sample 2 and sample 3 are base layers (the base layer is the garment worn under the PPE). Sample 4 to sample 7 are various types of outer or thermal layer fabrics used in FF PPE. The outer layer resists punctures and abrasions; and the thermal layer is for heat protection. Sample 8 is nanomaterial (nanofabric). The thicknesses were measured by SEM.

From these results, the nanofabric (sample 8, ~0.03 mm thick) lasted at least 4 min, which is longer than traditional FF fabric (**Fig. 5**). The flame test results are qualitative because the fabrics tested have different thicknesses and some samples may have

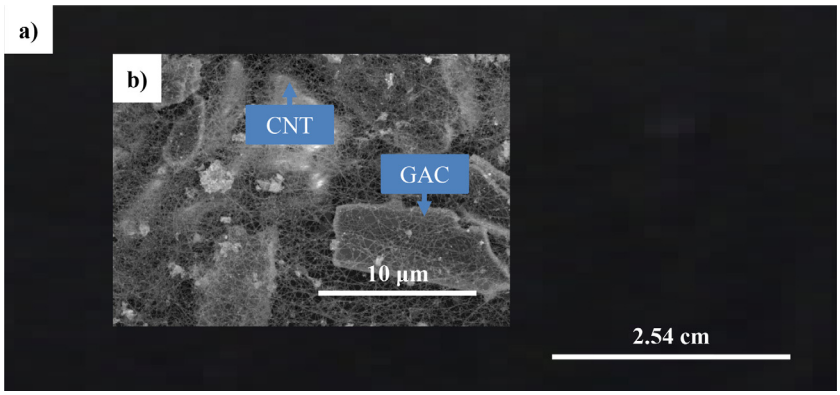

Fig. 3. CNT hybrid sheet characterization. (a) Nanofabric sheet and (b) SEM image of nanofabric. Both CNT and GAC are observed. The CNT bundles (hair-like sticks) are intertwined around the GACs (large partilces).

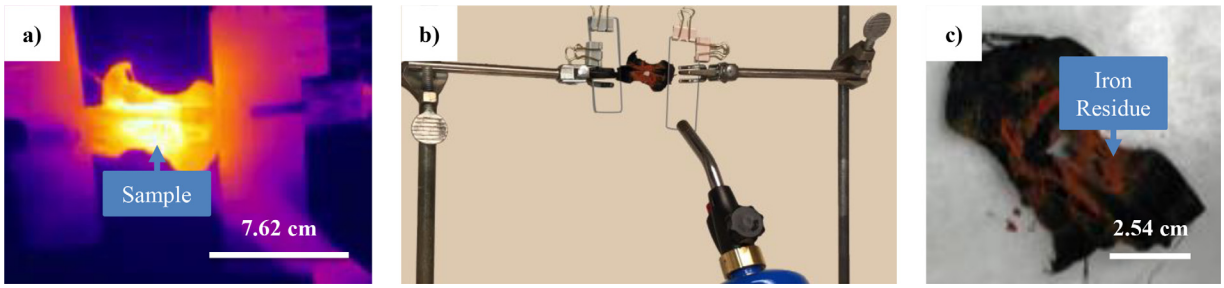

Fig. 4. Flammability test of nanofabric. (a) During and (b) after propane torch test. (c) Test result of nanofabric. (The iron residue has the appearance of rust.).

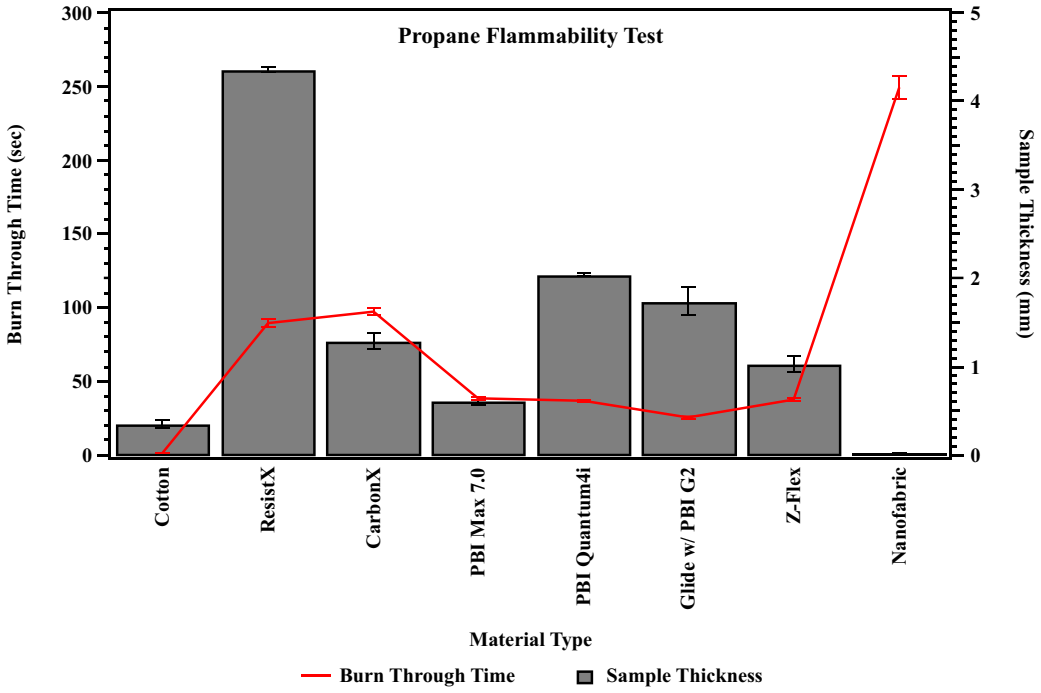

Fig. 5. Flame test results. Burn-through test time (line) vs sample thickness (bar).

Table 2
Propane flammability test results. Textile image of before and after test, description, thickness, and burn-through time are given in minutes to seconds (mm:ss).

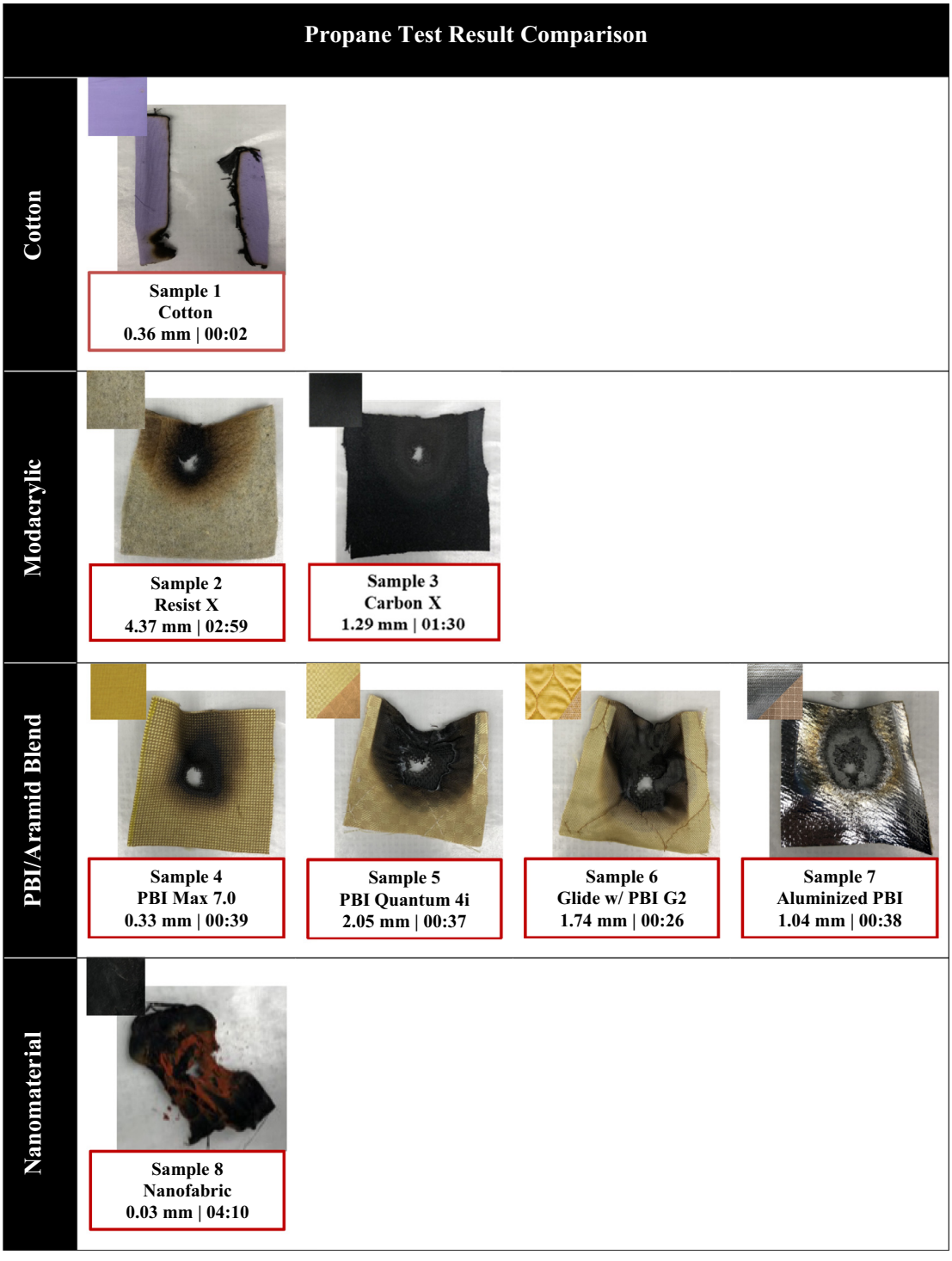

moved away from the flame due to the gas pressure during testing. If the sample surface moves away from the flame, the burn through time will increase.

3.2. Wettability testing

The wettability process uses a water droplet (of microliter size). The drop is held at the end of a syringe to avoid immediately running off the surface. The wetting property was determined by a direct measurement of contact angle, θ, by viewing the drop profile (**Fig. 6**). According to Himma et al. [29] there are five stages of wetting: 1) $\theta \cong 0°$ (superhydrophilic); 2) $0° \geq \theta \leq 90°$ (hydrophilic); 3) $90° < \theta \leq 120°$ (hydrophobic); 4) $120° \geq \theta \leq 150°$ (ultrahydrophobic); and 5) $\theta > 150°$ (superhydrophobic). Results of the contact angle test are shown in **Fig. 7**. Cotton, Quantum 4i, and Glide w/ PBI G2 fabrics were superhydrophilic to hydrophilic based on the contact angle, which took 24.8 s, 5 s, and 93.5 s, respectively, for water to be absorbed. Cotton and Glide w/ PBI G2

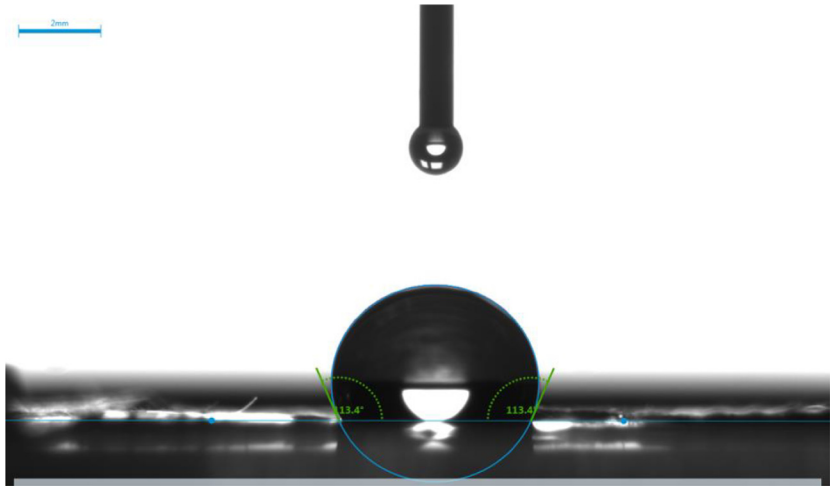

Fig. 6. Contact angle test of pristine nanofabric using water, $\theta = 113°$.

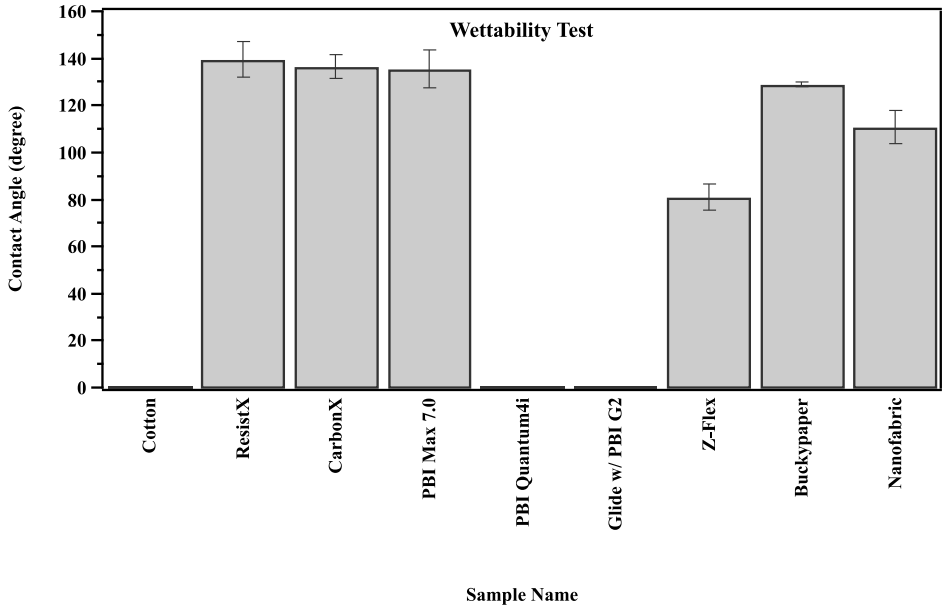

Fig. 7. Wettability of different fabrics.

had higher surface tension between the water droplet and surface than Quantum 4i. In addition to the surface tension, Glide w/ PBI G2 took longer for the water droplet to be absorbed because it had to break the tension between three separate layers. Z-flex is hydrophilic. Nanofabric, ResistX, CarbonX, and PBI Max 7.0 had $\theta > 90°$. However, Nanofabric's contact angle $\theta < 120°$ and thus the material is less hydrophobic.

3.3. Filter testing

Plastic furniture made from polyurethane (PU), nylon, and polyacrylonitrile (PAN) when burned can produce hydrogen cyanide as a by-product. Polyvinylchloride (PVC) made of chlorine, bromine, or fluorine – can release hydrochloric acid (HCl), hydrofluoric acid (HF), or hydrobromic acid (HBr) [30–32] when burned. Asphyxiation (short-term) and/or irritation (long-term) are possible side effects which could occur from these toxic chemical gasses (generated from combustion) if proper PPE isn't worn. Exposure to other potential chemicals that could cause long-term effects are metals, particulates, polycyclic aromatic hydrocarbons (PAHs), perfluorooctanesulfonates (PFOS), polychlorinated and polybrominated dioxins and furans (PCDD/PCDF, PBDD/PBDF, respectively) [32]. There are five main [sub]structures of polyaromatic hydrocarbons (listed in **Table 3**). It was reported that FFs are at least 5.5 times more susceptible than the average person for particles to be inhaled through or absorbed/adsorbed through the skin [32, 33].

Particulate filtration testing was performed on nanofabric and hybrid nanofabric as a filter. Air flow passes over the nanofabric and smoke particles and toxic chemicals adhere to the surface of the nanofabric (experimental setup for the test is shown in **Fig. 8a**). At high resolution (shown in **Fig. 9b-d**), nanofabric is a nonwoven sheet made of randomly oriented CNT bundles. The addition of GAC creates porosity in the sheet that enables breathability and filtering. Activated carbon air filters, consisting of a system of pores of varying molecular size, are the most effective type of filter against chemicals, gasses, smoke, and odors. An example of GAC is charcoal. When heated and treated with oxygen, millions of tiny pores appear. The pores can be highly absorbent by forming strong chemical attraction to contaminates (especially organic compounds). Thus, hybrid nanofabric will be a highly effective fil-

Table 3
List of carcinogenic polycyclic aromatic hydrocarbons.

Chemical	Formula	Structure	Raman Shift [cm^{-1}]				Ref
Anthracene	$C_{14}H_{10}$		756	1408	1563	–	[34, 38]
Fluorene	$C_{13}H_{10}$		373	1575	1616	1690	[36, 39]
Naphthalene	$C_{10}H_8$		1344	1577	–	–	[34, 35]
Phenanthrene	$C_{14}H_{10}$		1036	1349	1440	3071	[37]
Pyrene	$C_{16}H_{10}$		1241	1408	1596	1658	[34, 35, 38]

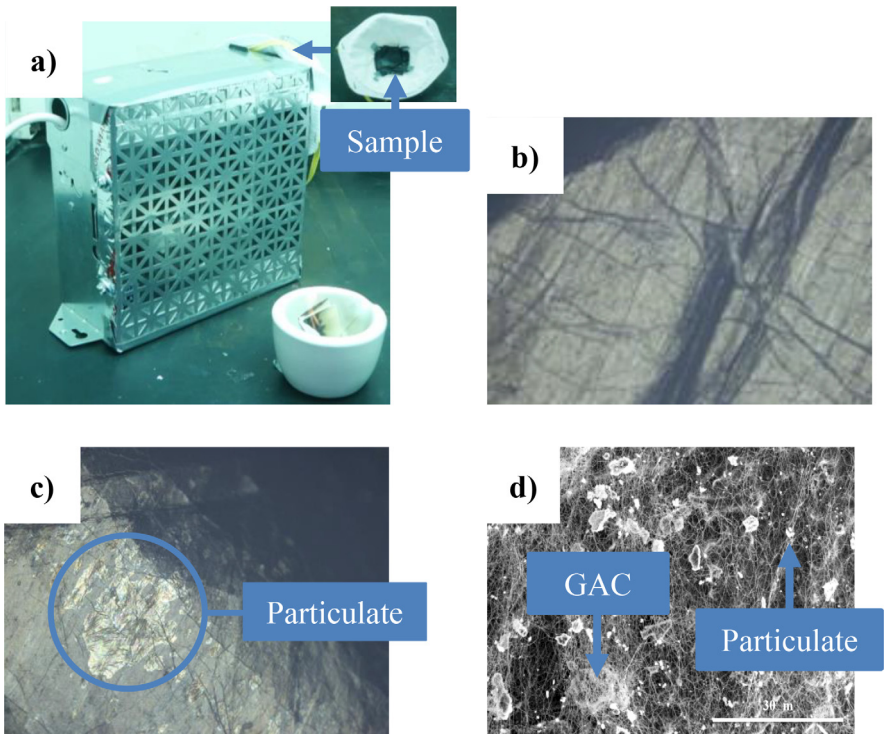

Fig. 8. Filtration test setup and results. (a) Experimental arrangement with a fan to draw smoke over a CNT sample. Smoke is generated from burning plastic. (b) Microscopy images of nanofabric before; and (c-d) after testing.

ter. To determine the effectiveness, microscopy (**Fig. 8c** and **d**) and Raman spectroscopy (**Fig. 9**) analyses were performed. After filtration, in **Fig. 8c**, there appears to be a crystalline compound absorbed onto the nanofabric.

Raman spectroscopy was performed before and after the filtration test to verify CNTs in the nanofabric – noted in three areas: 1) radial breathing mode (RBM) at 150 – 250 cm^{-1}; 2) defect peak (D peak) at 1355 cm^{-1}; and 3) graphitic peak (G peak) at 1550 – 1600 cm^{-1} [40, 41] shown in **Fig. 9**a [42]. From our analysis, the spectra shows a similar trend (shown in **Fig. 9**a and b), an increase in intensity at about 1600 ± 20 cm^{-1} is likely indicative of "C = C bond stretching motion" [41]. Thus, this suggests toxic gasses or particulates may have absorbed into the nanofabric surface after testing.

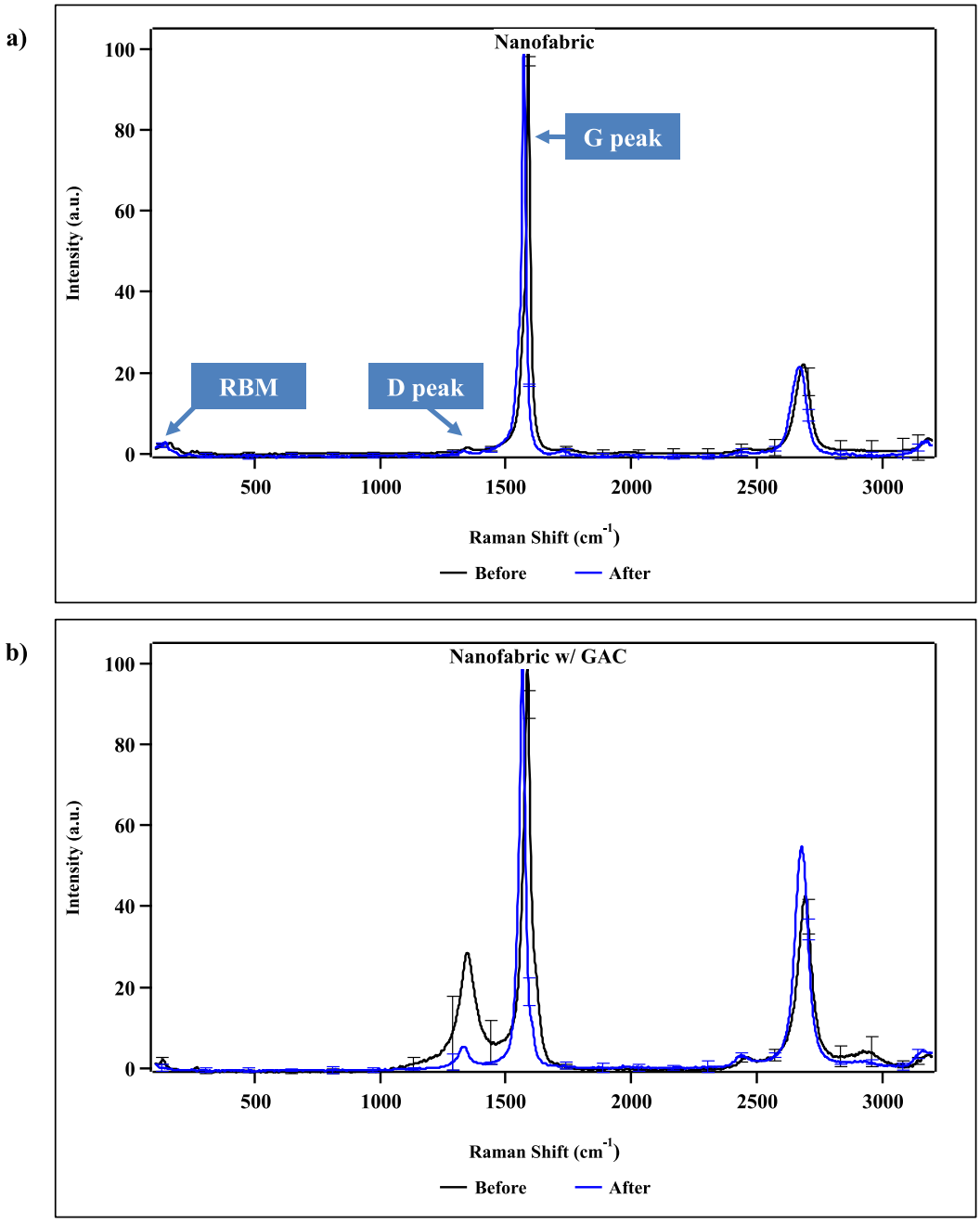

Fig. 9. Raman spectrum of before (black line) and after (blue line) filtering test of (a) nanofabric and (b) nanofabric with GAC.

4. Discussion

The flame resistance testing performed provided qualitative values of the flame resistance for different fabric materials. The testing is qualitative because of the test configuration and thicknesses of the samples used. This configuration has the fabric sample held in the vertical position and the flame perpendicular to the sample, which simulates the conditions in a firefighting environment. However, variations in the test configuration may produce differences in the burn-through time to some degree. The variations may occur for several reasons as explained. The first is in the test setup, the samples were not held against a surface allowing the sample to wrinkle or deform, thus possibly affecting the distance of the sample to the flame tip. Secondly, a slight variation in the position of the flame tip will affect the temperature of the flame on the fabric and the burn-through time. Thirdly, the flame gas pressure from the torch may cause the sample to move slightly away from the flame, reducing the temperature of the flame on the sample thus increasing the burn-through time. Fourthly, the samples were of different thicknesses due to the availability and construction of the fabric samples from the manufacturer. Layering fabric to achieve similar thickness for all samples was not performed as it could introduce issues of the layers delaminating/separating and add thermal barriers at the interfaces between the layers in the samples. The samples also have different coefficients of thermal expansion. The thermal expansion of nanotube fabric (due to the slight negative coefficient of thermal expansion for graphite) may affect the tension in the fabric when heated and allow the fabric to relax or warp. This may affect the temperature of the flame tip on the fabric and the burn-through time. In addition, it is not known how the sample thickness affects the burn-through time.

A new normalized parameter was defined called the burn-through parameter (sample thickness divided by the burn-through time, m/s). In future work, it is desired to derive a function that describes the burn-through parameter for specific fabric materials. This function may not be linear for certain materials such as nanotube fabric. Another possible reason for variation in results is that the flame temperature may affect the burn-through parameter. If the flame temperature is slightly above the burning temperature of the sample, the burn-through time could be longer. If the temperature is increased, the burn-through time may decrease dramatically. Thus, testing the samples that burn at different temperatures may produce different relative burn-through times depending on the flame temperature. As an extreme example, at a low flame temperature, cotton will still burn-through, but nanotube fabric may not burn-through for a very long time. At a high flame temperature, the burn-through times for cotton and nanotube fabric may be closer.

The very high-quality nanotube fabric tested here is more flame resistant than conventional fabric. We speculate there are several reasons why high-quality nanotube fabric has greater flame resistance than that of conventional. First, the nanotube fabric has a good thermal conductivity in the plane of the fabric. The good thermal conductivity spreads heat away from the point where the flame impinges on the fabric. If the fabric is cooler at the flame contact point, the burn-through time will be longer. Second, nanotube fabric contains about 20% by weight of iron catalyst on the inside and outside of nanotubes. Under the flame, the iron oxidizes and forms a secondary phase ceramic or refractory oxide material that is very flame resistant. The orange color in Fig. 4c shows the iron oxide. The iron oxide resists burning and increases the burn-through time. Third, the nanotube sample was much thinner (30 μm) than all the other sample materials. It is not known how the thickness of the nanotube fabric affects the burn-through time. Nanotube fabric spreads heat from a hot spot by conduction locally, then by convection. Thus, a thin nanotube fabric sample will spread heat locally at the flame tip by conduction, and then adjacent to the flame tip by convection, and overall cools very fast. Radiation heat transfer is also significant. Therefore, different thicknesses of nanotube fabric should be tested in the future and a burn-through rate function determined. Minimizing and optimizing the thickness of nanotube fabric to be used in FF garments is important to reduce the amount of fabric material used and to reduce the cost of the garment.

5. Summary and conclusion

Carbon nanofabric, pristine and hybrid (with GAC) material, was synthesized using a special gas phase pyrolysis process. Microscopy images of the hybrid nanofabric showed GAC in the nanofabric. The pristine fabric resisted the penetration of water and resisted burning. In addition, both fabric pristine and with GAC captured particulates. The nanofabric lasted longer than traditional samples before burning through the sample during flame testing. Further studies are needed to optimize carbon nanofabric mass production and to investigate in detail the safety of the nanofabric when used in FF apparel.

Supporting information

Carbon Nanofabric_Supporting Information

Declaration of Competing Interest

The authors declare that they have no known competing financial interests or personal relationships that could have appeared to influence the work reported in this paper.

The authors declare the following financial interests/personal relationships which may be considered as potential competing interests:

Acknowledgements

This research study is supported by the National Institute for Occupational Safety and Healt (NIOSH) through the University of Cincinnati Education Research Center (ERC) Grant #T42OH008432 (Pilot Research Project Training Program and Occupational Safety Health Engineering Fellowship). It was, also, broadly supported by ONR Award #N00014–15–1–2473 and I-Corps@Ohio 2017 Cohort. We would also like to thank Yoontaek Oh for his help in contact angle measurement.

Supplementary materials

Supplementary material associated with this article can be found, in the online version, at doi:10.1016/j.cartre.2022.100165.

References

[1] M. Wagner, L. Sullivan, The Columbus Dispatch, (Website) http://gatehousenews.com/unmasked/, 2017.
[2] DuPont, DuPont, Wilmington, D.E., USA (Website) http://hazard.com/msds/mf/dupont/nomex.html, 1991.
[3] FirefighterCancerSupportNetwork, (Website) http://mnfireinitiative.com/wp-content/uploads/2018/02/taking-action-against-cancer-in-the-fire-service-pdf.pdf, 2013.
[4] R.D. Daniels, T.L. Kubale, J.H. Yiin, M.M. Dahm, T.R. Hales, D. Baris, S.H. Zahm, J.J. Beaumont, K.M. Waters, L.E. Pinkerton, Occupational and Enviromental Medicine (OEM) (2013).
[5] R.D. Daniels, S. Bertke, M.M. Dahm, J.H. Yiin, T.L. Kubale, T.R. Hales, D. Baris, S.H. Zahm, J.J. Beaumont, K.M. Waters, L.E. Pinkerton, Occupational and Enviromental Medicine (OEM) (2015).
[6] J.R. Brown, B.C. Ennis, Text. Res. J. 47 (1977) 62–66.
[7] B. Yu, International Fabricare Instittute, (Website) 70.88.161.72/ifi/BULLETIN/FF/Ff394.pdf, 1991.
[8] R.H. Jackson, Text. Res. J. 48 (1978) 314–319.
[9] PBI.PerformanceProducts, PBI Performance Products, INC., (Website) https://pbiproducts.com/fabrics/why-choose-pbi/, 2018.
[10] IFSTA, FPP, Essentials of Fire Fighting, 6th Ed., 6 ed., Fire Protection Publications (FPP)/International Fire Service Training Association (IFSTA), Stillwater, OK (Website) https://www.ifsta.org/shop/essentials-fire-fighting-6th-edition/36922?gclid=EAIaIQobChMI7ZDz7aDE2wIVC0JpCh21ZwwDEAMYASAAEgI9TfD_BwE, 2013.
[11] DuPont, DuPont, Wilmington, D.E., USA (Website) http://www.dupont.com/content/dam/dupont/products-and-services/personal-protective-equipment/thermal-protective-apparel-and-accessories/documents/DPT_Nomex_Laundering_Guide.pdf, 1997.
[12] W.E. Clark, Chapter 8. Safety on the Fireground, Firefighting Principles and Problems, Fire Engineering Books & Videos, Saddle Brook, NJ, 1992, pp. 171–204.
[13] R.F. Fahy, P.R. LeBlanc, J.L. Molis, (Website) https://www.nfpa.org/-/media/Files/News-and-Research/Fire-statistics/Fire-service/osFFF.pdf, 2018.
[14] Handbook of Fire Resistant TextilesWoodhead Publishing Limited, 1 ed., The Textile Institute, Philadelphia, PA, USA Cambridge, UK, 2013.
[15] R.M. Rossi, Chapter 15. Characterizing Comfort Properties of Flame Resistant Fabrics and Garments, in: F.S. Kilinc (Ed.), Handbook of Fire Resistant Textiles, Woodhead Publishing Limited in association with The Textile Institute Woodhead Publishing Limited, Philadelphia, PA, 2013, pp. 415–433.
[16] NIOSH, (Website) https://www.cdc.gov/niosh/fire/reports/face201117.html, 2012.
[17] S. Mandal, G.u. Song, J. Ind. Text. 47 (2018) 622–639.
[18] W.E. Mell, R. Lawson, Fire Technol. 36 (2000) 39–68.
[19] F. Wang, K. Kuklane, C. Gao, I. Holmér, Physiol. Meas. 32 (2011) 239–249.
[20] S.S. Bruce-Low, D. Cotterrell, G.E. Jones, Ergonomics 50 (2007) 80–98.
[21] D. Janas, M. Rdest, K.K.K. Koziol, Mater. Des. 121 (2017) 110–125.
[22] X. Wang, E.N. Kalali, J.-.T. Wan, D.-.Y. Wang, Prog. Polym. Sci. 69 (2017) 22–46.
[23] K. Aschberger, I. Campia, L.Q. Pesudo, A. Radovnikovic, V. Reina, Environ. J. 101 (2017) 27–45.
[24] C. Dewaghe, C.Y. Lew, M. Claes, S.A. Belgium, P. Dubois, 23 - Fire-Retardant Applications of Polymer–Carbon Nanotubes Composites: improved Barrier Effect and Synergism, in: T. McNally, P. Pötschke (Eds.), Polymer–Carbon Nanotube Composites, Woodhead Publishing, 2011, pp. 718–745.
[25] A. International, ASTM International, West Conshohocken, PA, 2018.
[26] G. Hou, R. Su, A. Wang, V. Ng, W. Li, Y. Song, L. Zhang, M. Sundaram, V.N. Shanov, D. Mast, D.S. Lashmore, M.J. Schulz, Y. Liu, Carbon N Y 102 (2016) 513–519.

[27] G. Hou, D. Chauhan, V. Ng, C. Xu, Z. Yin, M. Paine, R. Su, V.N. Shanov, D. Mast, M.J. Schulz, Y. Liu, Mater. Des. 132 (2017) 112–118.
[28] A. International, ASTM International, West Conshohocken, PA, 2013.
[29] N.F. Himma, N. Prasetya, S. Anisah, I.G. Wenten, Rev. Chem. Eng. 35 (2019) 211–238.
[30] W.D. Woolley, S.A. Ames, P.J. Fardell, Fire Mater. 3 (1979) 110–120.
[31] I.S. Wichman, Prog. Energy Combust. Sci. 29 (2003) 247–299.
[32] A.A. Stec, K.E. Dickens, M. Salden, F.E. Hewitt, D.P. Watts, P.E. Houldsworth, F.L. Martin, Sci. Rep. 8 (2018) 2476.
[33] S. Smith, EHS Today 2017.
[34] H. Shinohara, Y. Yamakita, K. Ohno, J. Mol. Struct. 442 (1998) 221–234.
[35] A.D. Chanyshev, K.D. Litasov, A.F. Shatskiy, I.S. Shargygin, Y. Higo, E. Ohtani, Phys. Earth Planet. Inter. 270 (2017) 29–39.
[36] W.C. Tsoi, D.G. Lidzey, J. Phys. Condens. Matter 20 (2008) 125213.
[37] A.I. Alajtal, H.G.M. Edwards, M.A. Elbagerma, I.J. Scowen, Spectrochim. Acta Part A 76 (2010) 1–5.
[38] X. Gu, S. Tian, Q. Zhou, J. Adkins, Z. Gu, X. Li, J. Zheng, RSC Adv. 3 (2013) 25989–25996.
[39] SpectraBase, John Wiley & Sons, Inc., [Website] https://spectrabase.com/spectrum/EKNHzNfFmYX, 2021, pp. 38.
[40] R. Saito, A. Grüneis, G.G. Samsonidze, V.W. Brar, G.F. Dresselhaus, M.S. Dresselhaus, A. Jorio, L.G. Cançado, C. Fantini, M.A. Pimenta, A.G. Souza Filh, New J. Phys. 5 (2003) 157.151-157.115.
[41] R. Saito, T. Takeya, T. Kimura, G.F. Dresselhaus, M.S. Dresselhaus, Phys. B Rev. 57 (1998) 4145–4153.
[42] S. Li, G. Chen, Y. Zhang, Z. Guo, Z. Liu, J. Xu, X. Li, L. Lin, Opt. Express 22 (2014).